



RSC Soft Matter Series

Non-wettable Surfaces

Theory, Preparation and Applications

Edited by Robin H. A. Ras and Abraham Marmur



Non-wettable Surfaces

Theory, Preparation and Applications

RSC Soft Matter Series

Series Editors:

Professor Dr Hans-Jürgen Butt, *Max Planck Institute for Polymer Research, Germany*

Professor Ian W. Hamley, *University of Reading, UK*

Professor Howard A. Stone, *Princeton University, USA*

Professor Chi Wu, *The Chinese University of Hong Kong, China*

Titles in this Series:

1: Functional Molecular Gels

2: Hydrogels in Cell-based Therapies

3: Particle-stabilized Emulsions and Colloids: Formation and Applications

4: Fluid-Structure Interactions in Low-Reynolds-Number Flows

5: Non-wettable Surfaces: Theory, Preparation and Applications

How to obtain future titles on publication:

A standing order plan is available for this series. A standing order will bring delivery of each new volume immediately on publication.

For further information please contact:

Book Sales Department, Royal Society of Chemistry, Thomas Graham House, Science Park, Milton Road, Cambridge, CB4 0WF, UK

Telephone: +44 (0)1223 420066, Fax: +44 (0)1223 420247

Email: booksales@rsc.org

Visit our website at www.rsc.org/books

Non-wettable Surfaces

Theory, Preparation, and Applications

Edited by

Robin H. A. Ras

Aalto University, Espoo, Finland

Email: robin.ras@aalto.fi

and

Abraham Marmur

Technion – Israel Institute of Technology, Haifa, Israel

Email: marmur@technion.ac.il



RSC Soft Matter No. 5

Print ISBN: 978-1-78262-154-6

PDF eISBN: 978-1-78262-395-3

EPUB eISBN: 978-1-78262-968-9

ISSN: 2048-7681

A catalogue record for this book is available from the British Library

© The Royal Society of Chemistry 2017

All rights reserved

Apart from fair dealing for the purposes of research for non-commercial purposes or for private study, criticism or review, as permitted under the Copyright, Designs and Patents Act 1988 and the Copyright and Related Rights Regulations 2003, this publication may not be reproduced, stored or transmitted, in any form or by any means, without the prior permission in writing of The Royal Society of Chemistry or the copyright owner, or in the case of reproduction in accordance with the terms of licences issued by the Copyright Licensing Agency in the UK, or in accordance with the terms of the licences issued by the appropriate Reproduction Rights Organization outside the UK. Enquiries concerning reproduction outside the terms stated here should be sent to The Royal Society of Chemistry at the address printed on this page.

The RSC is not responsible for individual opinions expressed in this work.

The authors have sought to locate owners of all reproduced material not in their own possession and trust that no copyrights have been inadvertently infringed.

Published by The Royal Society of Chemistry,
Thomas Graham House, Science Park, Milton Road,
Cambridge CB4 0WF, UK

Registered Charity Number 207890

For further information see our web site at www.rsc.org

Printed in the United Kingdom by CPI Group (UK) Ltd, Croydon, CR0 4YY, UK

Preface

This book is about a topic that has been known for many decades. However, it has become extremely popular only during the last two decades. We do not know what the reason is—maybe the very successful association with the purity and cleanliness of the lotus. However, we are happy it happened, since it is a challenging as well as rewarding topic, both theoretically and practically.

This book attempts to cover the whole spectrum, from the theoretical fundamentals to the practical applications of non-wettable surfaces. Although thousands of papers have been published, mainly on various production methods, many pieces of the puzzle are still missing. The most obvious missing part is the problem of long-term durability, which may be the main reason why superhydrophobic consumer products are not yet common. There are also some differences of opinion with regard to theoretical aspects, and even terminology. We very much hope that this book will be not only a source of knowledge, but also a catalyst for future development.

Robin Ras
Abraham Marmur

Contents

Chapter 1	Non-Wetting Fundamentals	1
	<i>Abraham Marmur</i>	
1.1	Introduction	1
1.2	Wetting Equilibrium	2
1.3	Mechanism and Definition of Non-Wettability	4
1.4	Stability Considerations	6
1.4.1	A Drop on a Non-Wettable Surface	6
1.4.2	Underwater Superhydrophobicity	9
1.5	Conclusions	10
	References	10
Chapter 2	Non-Wetting, Stabilization, and Phase Transitions Induced by Vibrations and Spatial Patterns	12
	<i>Rahul Ramachandran and Michael Nosonovsky</i>	
2.1	Introduction	12
2.2	Effective Force Corresponding to Small Fast Vibrations	14
2.2.1	Motion Subjected to a Rapidly Oscillating Force	14
2.2.2	Inverted Pendulum	17
2.2.3	Mathieu Equation Method	19
2.2.4	Multiple Pendulums and the Indian Rope Trick	20
2.3	Vibro-Levitation of Droplets	25
2.3.1	Vibro-Levitating Droplets and Inverted Pendulum	27

2.3.2	Experimental Study	29
2.3.3	Results	29
2.4	Vibration and Phase Transition	30
2.4.1	Effective Freezing	31
2.4.2	Cornstarch Monsters	31
2.4.3	Effective Liquid Properties and Surface Tension of Granular Materials	32
2.4.4	Locomotion in a Viscous Liquid	33
2.5	Surface Texture-Induced Phase Transitions	33
2.5.1	Kirchhoff's Analogy	35
2.5.2	Surface Texture-Induced Superhydrophobicity	36
2.5.3	Surface Texture-Induced Phase Transitions	37
2.6	Conclusions	38
	References	39
Chapter 3	Superoleophobic Materials	42
	<i>Thierry Darmanin and Frédéric Guittard</i>	
3.1	Introduction	42
3.2	Superoleophobicity Theories	43
3.3	Fabrication of Superoleophobic Materials	45
3.3.1	Plasma Etching/Reactive Ion Etching	45
3.3.2	Chemical Etching	46
3.3.3	Galvanostatic Deposition	50
3.3.4	Anodization	51
3.3.5	Use of Nanoparticles	53
3.3.6	Hydrothermal and Solvothermal Processes	57
3.3.7	Chemical Vapour Deposition	59
3.3.8	Electrodeposition	59
3.3.9	Electrospinning	61
3.3.10	Layer-by-Layer Deposition	63
3.3.11	Lithography	63
3.3.12	Use of Textured Substrates	69
3.4	Conclusion	72
	References	72
Chapter 4	Liquid-Repellent Nanostructured Polymer Composites	84
	<i>Ilker S. Bayer</i>	
4.1	Introduction	84
4.2	Polymer Coatings	85
4.2.1	Fluoropolymer Matrix Polymer Composites	88
4.2.2	Silicone Matrix Polymer Composites	96

4.2.3	Wear Abrasion Resistant Liquid-Repellent Polymer Composites	104
4.2.4	Environmentally Friendly Processes and Materials for Liquid-Repellent Polymer Composites	109
4.3	Conclusions	115
	References	115
Chapter 5	Etching Techniques for Superhydrophobic Surface Fabrication	117
	<i>Sami Franssila</i>	
5.1	Introduction	117
5.2	Plasma Etching	118
5.2.1	Basics	118
5.2.2	Limitations in Plasma Etching	122
5.2.3	DRIE for Shapes Other than Pillars	123
5.2.4	Nanoroughness by Non-Masked Plasma Etching	124
5.3	Silicon Anisotropic Wet Etching	127
5.3.1	Silicon Nanostructures by Metal-Assisted Wet Etching	129
5.4	Combined Processes	131
5.5	Plasma Etching for Polymer Master Mould Fabrication	134
5.6	Glass Plasma Etching	135
5.7	Polymer Plasma Etching	137
5.8	Plasma Etcher as a Deposition Tool	138
5.9	Conclusions	139
	References	140
Chapter 6	Design Principles for Robust Superoleophobicity and Superhydrophobicity	145
	<i>Kock-Yee Law and Hong Zhao</i>	
6.1	Introduction	145
6.2	Study of a Model Superoleophobic Surface	147
6.2.1	Fabrication and Characterization of a Model Textured Surface	147
6.2.2	Basic Design Parameters for Superoleophobicity	148
6.2.3	Composite Liquid-Solid-Air Interface and Pinning Location	152
6.3	Robust Design Parameters for Superoleophobicity	154
6.3.1	Robustness Study on Wettability, Adhesion, and Hysteresis	156

6.3.2	Effect of Wavy Structure on Wetting Stability	158
6.3.3	Effect of Re-Entrant Geometry on Wetting Stability	163
6.3.4	Effect of Breakthrough Pressure on Superoleophobicity	164
6.3.5	Mechanical Robustness Against Abrasion	166
6.3.6	Design Space and Latitude for Robust Superoleophobicity	168
6.4	Discussion of Robust Design Parameters for Superhydrophobicity	170
6.4.1	Re-Entrant and Overhang Structures	170
6.4.2	Hierarchical, Multi-Scale Roughness	171
6.4.3	Design Parameters for Robust Superhydrophobicity	172
6.5	Summary and Remarks	173
6.5.1	Gaps in Product Features and Measurements	174
6.5.2	Compromises and Trade-Off	174
6.5.3	Challenges in Manufacturing	177
6.5.4	Concluding Remarks	178
	Acknowledgements	179
	References	179
Chapter 7	Patterned Superhydrophobic Surfaces	182
	<i>Erica Ueda and Pavel A. Levkin</i>	
7.1	Introduction	182
7.2	Fabrication of Surfaces with Patterned Wettability	183
7.2.1	UV Light Irradiation	183
7.2.2	Phase Separation and UVO Irradiation	184
7.2.3	Hydrophilic–Superhydrophobic Black Silicon Patterned Surfaces	184
7.2.4	UV-Initiated Free Radical Polymerization and Photografting	185
7.2.5	Surface Patterning <i>Via</i> Thiol-yne Click Chemistry	186
7.2.6	Surface Functionalization <i>Via</i> Thiol-ene Reaction	189
7.2.7	Surface Functionalization <i>Via</i> UV-Induced Tetrazole–Thiol Reaction	189
7.2.8	Surface Modification Through Polydopamine	190
7.2.9	Superomniphobic–Superomniphilic Patterned Surfaces	191
7.2.10	Amine-Reactive Modification of Superhydrophobic Polymers	192
7.2.11	Patterns of Reversible Wettability	192

7.3 Applications of Patterned Superhydrophobic Surfaces	194
7.3.1 Open Microfluidic Channels	194
7.3.2 Cell Patterning and Cell Microarrays	196
7.3.3 Cell or Chemical Screening in Arrays of Liquid or Hydrogel Droplets	199
7.3.4 Positioning or Sorting Particles	204
7.3.5 Self-Assembly of Microchips	208
7.3.6 Lithographic Printing	208
7.3.7 Patterning Textiles	210
7.3.8 Patterning Slippery Lubricant-Infused Porous Surfaces	211
7.3.9 Fog Collection	214
7.3.10 Heat Transfer During Boiling	217
7.4 Conclusions	217
Acknowledgements	218
References	218
Chapter 8 Natural and Artificial Surfaces with Superwettability for Liquid Collection	223
<i>Jie Ju, Xi Yao and Lei Jiang</i>	
8.1 Introduction	223
8.2 Liquid Collection on Natural and Artificial Desert Beetles	224
8.2.1 Liquid Collection on Natural Desert Beetles	224
8.2.2 Surfaces with Patterned Wettability Used for Dew Collection <i>Via</i> Subcooling Condensation	225
8.2.3 Artificial Surfaces with Patterned Wettability Used for Liquid Collection <i>Via</i> Fog Deposition	227
8.3 Liquid Collection on Natural and Artificial Spider Silks	229
8.3.1 Liquid Collection on Natural Spider Silks	230
8.3.2 Liquid Collection on Artificial Spider Silks with Uniform Spindle-Knots	231
8.3.3 Artificial Spider Silks with Non-Uniform Spindle-Knots for Liquid Collection	236
8.4 Liquid Collection on Natural and Artificial Cactus	238
8.4.1 Liquid Collection on Natural Cactus	238
8.4.2 Liquid Collection on Artificial Cactus	240
8.4.3 Artificial Cactus for Oil/Water Separation	243
8.5 Other Kinds of Surfaces with Superwettability for Directional Liquid Collection	244
8.5.1 Natural Surfaces with Superwettability for Liquid Collection	245
8.5.2 Artificial Surfaces with Superwettability for Liquid Collection	247

8.6 Conclusion and Outlook	249
References	249
Chapter 9 Wetting Properties of Surfaces and Drag Reduction	253
<i>Glen McHale</i>	
9.1 Introduction	253
9.1.1 Superhydrophobicity, Leidenfrost Effect, and SLIPS/LIS Surfaces	253
9.1.2 Importance of Vapour/Fluid Interfaces	254
9.1.3 Literature Reviews	255
9.1.4 Types of Experimental Methods	256
9.1.5 Retention and Generation of Gas/Vapour Layers	257
9.2 Velocity Profiles Near Surfaces and Slip	258
9.2.1 Slip Velocity, Slip Length and Friction	258
9.2.2 Apparent Slip and Lubricating Surface Flows	259
9.2.3 Molecular Slip and Equilibrium/Dynamic Contact Angles	261
9.2.4 Slip and Surface Texture	262
9.2.5 Effective Slip and Mixed Boundary Conditions	264
9.3 Internal Flow Through Pipes	265
9.3.1 Navier–Stokes Equations and Reynolds Number	265
9.3.2 Poiseuille Flow and Friction Factor	266
9.3.3 Apparent Slip, Core Annular Flow, and Net ZMF Condition	268
9.4 External Flow Past Cylinders and Spheres	271
9.4.1 Pressure and Form Drag	271
9.4.2 Coefficient of Drag and Types of Flow Patterns	272
9.4.3 Stokes with Slip and Hadamard–Rybczinski Drag for Spheres	274
9.4.4 Plastron Drag Reduction for Spheres	275
9.4.5 Plastrons and Vortex Suppression	277
9.5 Summary	278
Acknowledgements	279
References	279
Chapter 10 Lubricant-Impregnated Surfaces	285
<i>Brian R. Solomon, Srinivas Bengaluru Subramanyam, Taylor A. Farnham, Karim S. Khalil, Sushant Anand and Kripa K. Varanasi</i>	
10.1 Introduction	285
10.2 Fundamentals	286

10.2.1	The Cloak	289
10.2.2	Wetting Ridge	291
10.2.3	Excess Films and Steady State	291
10.3	Applications	292
10.3.1	Condensation	292
10.3.2	Anti-Icing	296
10.3.3	Anti-Fouling	299
10.3.4	Fluid Mobility	303
10.3.5	Active Surfaces	306
10.3.6	Optics	307
10.3.7	Infused Gels	307
10.3.8	Durability	308
10.4	Conclusion and Outlook	310
	References	311
Chapter 11	Fundamentals of Anti-Icing Surfaces	319
	<i>Alidad Amirfazli and Carlo Antonini</i>	
11.1	Introduction	319
11.2	How Surfaces Can Be Used to Help with Icing—Icephobicity <i>Versus</i> Superhydrophobicity	321
11.3	Fundamental Concepts of Ice Nucleation	323
11.3.1	Homogeneous Freezing	324
11.3.2	Heterogeneous Freezing	326
11.4	The Role of Surface Properties and of the Environment in Icing	327
11.4.1	Surface Wetting	327
11.4.2	Textured or Rough Surfaces	329
11.4.3	Environmental Conditions	331
11.5	Water and Ice Interaction with Surfaces in Icing Conditions	332
11.5.1	Dynamic Water–Surface Interaction in Icing Conditions	332
11.5.2	Ice Adhesion on Anti-Icing Surfaces	339
11.6	Alternative Routes: Soft Surfaces and Biomimicry of the Antifreeze Protein	342
11.7	Surface Durability Considerations	342
11.8	Conclusions	343
	References	343
Chapter 12	Oil–Water Separation with Selective Wettability Membranes	347
	<i>Ethan Post, Gibum Kwon and Anish Tuteja</i>	
12.1	Introduction	347
12.2	Fundamentals of Wettability	348

12.3	Design Strategies for Composite Membranes with Selective Wettability	351
12.4	Membranes with Selective Wettability	354
12.4.1	Hydrophobic and Oleophilic Membranes	354
12.4.2	Hydrophilic and Oleophilic Membranes	357
12.4.3	Hydrophilic and Oleophobic Membranes	359
12.4.4	Hydrophobic and Oleophobic Membranes	361
12.5	Conclusions and Future Outlook	362
	Acknowledgements	362
	References	362
Chapter 13	Droplet Manipulation on Liquid-Repellent Surfaces	368
	<i>Robin H. A. Ras, Xuelin Tian, Bo Chang and Jaakko V. I. Timonen</i>	
13.1	Droplet Friction	368
13.2	Gravity-Induced Droplet Manipulation	373
13.3	Magnetic Field-Induced Droplet Manipulation	376
13.3.1	Magnetic Droplets Based on Non-Uniformly Dispersed Magnetic Particles	377
13.3.2	Magnetic Droplets Based on Uniformly Dispersed Magnetic Nanoparticles	377
13.3.3	Magnetically Controllable Superhydrophobic Surfaces	379
13.3.4	Other Systems	381
13.4	Conclusions	381
	References	382
	Subject Index	385

CHAPTER 1

Non-Wetting Fundamentals

ABRAHAM MARMUR^a

^aChemical Engineering Department, Technion – Israel Institute of Technology, Haifa 3200003, Israel

*E-mail: marmur@technion.ac.il

1.1 Introduction

Wetting is a ubiquitous process that occurs in a huge variety of everyday biological and industrial systems. It is a macroscopic process that is very sensitive to surface properties on the nano or molecular scale. In most wetting situations the solid surface is wet only to some extent, depending on its chemical and physical nature. As is well known, the common quantitative measure of wettability is the contact angle (CA), which in most cases is greater than 0° and much less than 180° . However, the extreme cases of either complete wetting (CA = 0°) or non-wetting (very high CA and additional possible criteria to be discussed below) offer interesting scientific challenges as well as practical applications. Actually, nature has been using non-wetting to solve a variety of important needs, and the main scientific principle has been known for about half a century.¹ However, it is only about two decades ago that it started to become a very popular topic in science and engineering.²⁻⁴⁶ The paper by Neinhuis and Barthlott³ served as an important trigger to the vast interest in non-wetting. It introduced the term “lotus effect” that refers to the self-cleaning of the lotus leaf (and many others), achieved by water drops easily rolling off the surface of the leaf, carrying with them dust and dirt particles.

RSC Soft Matter No. 5

Non-wettable Surfaces: Theory, Preparation, and Applications

Edited by Robin H. A. Ras and Abraham Marmur

© The Royal Society of Chemistry 2017

Published by the Royal Society of Chemistry, www.rsc.org

However, non-wettability is relevant not only for self-cleaning of leaves and not only for drops. For example, some aquatic animals breathe air from an air film on their body even when they are under water. This air film is re-created each time the animal goes back into the water.*e.g.*^{24,36} In addition, while natural systems are predominantly aqueous, the non-wettability of solid surfaces by oils, or organic liquids in general, is also of great practical importance in daily life and in industry.^{25,26}

At this point it is important to discuss terminology,^{25,41} since there is no standard one and the variety of terms may lead to confusion. A surface that is not wetted by water drops in air, or may sustain an air film under water, is in many cases classified as “water repellent”. This usage is unfortunate, because there is nothing active in this process that repels water. The adjective “non-wettable” (or the noun “non-wetting”), on the other hand, appears to be more true to the facts. Moreover, the so-called “water repellent” surfaces are usually classified as “superhydrophobic”. However, when a surface is not wetted even by liquids of lower surface tension than of water, this term cannot be used, since “hydro” specifically means water. For this purpose, other terms are used, seemingly at random. One term is “superoleophobic”. This is a problematic term, since a surface that is “superoleophobic” is usually also superhydrophobic, so “oleophobic” refers only to a part of the picture. On the other hand, a term such as “omniphobic”, which means “fearing everything”, is far too wide, since, after all, the discussion is about liquids, not about everything. Some time ago I suggested^{25,42} using the term “superhygrophobic” to imply non-wetting, because “hygro” in Greek means “liquid”. Thus, the terms “hygrophobic” and “superhygrophobic” exactly express various degrees of non-wetting by liquids in general. In summary, “non-wetting” is a generic term that may be specifically complemented by “superhydrophobic” or “superhygrophobic” when it is important to know what the specific case is.

In order to develop useful non-wettable surfaces, it is important to understand the fundamental theory and apply it in choosing the chemical and physical properties of the surfaces. The objective of this chapter is to present the thermodynamic fundamentals of non-wetting, as they are derived from the general theory of wetting equilibrium. An important aspect that has not been sufficiently noticed and is emphasized here is that of thermodynamic stability. In general, qualitative aspects are stressed in this chapter, with only a few necessary equations, in order to give the general picture rather than the mathematical details.

1.2 Wetting Equilibrium

As is well known, minimizing the energy of a system (internal, Gibbs, or Helmholtz energy, depending on the conditions at the system boundary) leads to a few indicators of equilibrium. First, for all systems, irrespective of the existence of interfaces, the temperature as well as the generalized chemical potential of each species must be uniform throughout the whole system. Then, there are two equations that govern the equilibrium state of an interface: the Young equation and the Young-Laplace equation. The former

determines the boundary condition for the shape of the liquid–gas interface, in terms of the local CA that must equal the Young CA, θ_Y . For solid–liquid–gas systems it is given by

$$\cos \theta_Y = (\sigma^s - \sigma^{sl})/\sigma \quad (1.1)$$

here, σ and σ^s are the surface tension of the liquid and of the solid, respectively, and σ^{sl} is the solid–liquid interfacial tension. This equation is correct for radii of curvature much above the nano scale, for which line tension is negligible *e.g.* ref. 47.

The Young–Laplace equation determines the shape of the interface, in terms of the local curvature that is determined by the local pressure difference across the interface:

$$P^d - P^c = \sigma(1/R_1 + 1/R_2) \quad (1.2)$$

in this equation, P^d and P^c are the local pressure in the drop and in the continuous phase, respectively, and R_1 and R_2 are the local radii of curvature. In the absence of gravity (or other external fields), the pressure difference is constant across the interface. This implies that the average curvature is also constant across the interface. This well-known fact is important for understanding the behaviour of liquids inside roughness grooves, as will be discussed later.

Eqn (1.1) and (1.2) completely determine the equilibrium behaviour of an interface. When the solid surface is ideal (*i.e.* rigid, smooth, chemically uniform, non-reactive, and insoluble) there is only one solution to these equations, which requires the apparent, namely macroscopically measured CA, to equal the Young CA. However, when the surface is rough or chemically non-uniform, there are many possible solutions. Each solution is characterized by its own apparent CA. Naturally, it is important and interesting to find out (a) which of these solutions has the lowest energy, namely which is the thermodynamically most stable CA, and (b) what are the lowest (receding) and highest (advancing) apparent CAs. The difference between the advancing and receding CAs is called the CA hysteresis range.

When a mathematical function has multiple minima, the only way to identify these minima is to search for them one by one. To find out the global minimum, it is necessary to compare all of them and identify the lowest. There is no general mechanism for this. Luckily, for wetting on rough or chemically heterogeneous surfaces, we have approximate equations for the most stable CA.^{1,47} The accuracy of these equations improves as the ratio of the radius of curvature to the heterogeneity scale increases.⁴⁹ For rough but chemically uniform surfaces we have the Wenzel equation,⁴⁸ which assumes the liquid to penetrate completely into the roughness grooves. This state will be referred to as the W state. The apparent CA associated with this global minimum, θ_w , is given by

$$\cos \theta_w = r \cos \theta_Y \quad (1.3)$$

in this equation, r is the roughness ratio, defined as the ratio between the true area of the solid surface and its projection on a horizontal surface. The above discussion of eqn (1.3) also holds for chemically heterogeneous surfaces. The most stable minimum in energy occurs at the angle that is given by¹

$$\cos \theta_c = x_1 \cos \theta_{Y1} + x_2 \cos \theta_{Y2} \quad (1.4)$$

here, x_1 and x_2 are the ratios of contact area of the solid with each chemistry to the projection of total area of the solid, and θ_{Y1} and θ_{Y2} are the Young CAs corresponding to the two chemistries. If the heterogeneous solid surface is flat, then $x_1 + x_2 = 1$; however it is >1 if the heterogeneous solid surface is also rough. We can easily generalize this equation to a higher number of chemistries, using the principle of linear averaging.

When the surface is rough, there may also be equilibrium positions associated with partial penetration of the liquid into the roughness grooves. This case was first studied by Cassie and Baxter,¹ therefore it is referred to as the CB state. The equation for the apparent CA in this case can be derived from eqn (1.3) and (1.4), assuming the solid surface to be represented by θ_{Y1} , and air (or an inert gas in general) to be represented by θ_{Y2} . Because of the perfect hydrophobicity of air, θ_{Y2} is taken to be 180° . The solid-liquid area per unit projection area is $r_f f$, where f is the area fraction of the projection of the wetted part of the solid surface, and r_f is the roughness ratio of the wetted solid. The liquid-gas interface within the roughness is assumed to be flat, therefore its true area fraction is well approximated by its projected area fraction, $(1 - f)$. The apparent flatness of the liquid-gas interface stems from the fact that the pressure inside the liquid is very nearly uniform (if the effect of gravity is small), therefore the radius of curvature around the liquid body must be uniform too. Since this radius of curvature is usually very large compared with the distance between the protrusions of the roughness, the liquid-gas interface inside the grooves appears to be almost flat. This theoretical conclusion^{12,25,29} has recently been demonstrated experimentally.⁵⁰ Substituting the above information into eqn (1.4), the CB equation reads

$$\cos \theta_{CB} = r_f f \cos \theta_{Y1} + (1 - f)(-1) = -1 + f(1 + r_f \cos \theta_{Y1}) \quad (1.5)$$

A common problem in publications is the omission of r_f . Assuming $r_f = 1$ is correct only if the roughness protrusions have flat tops that are parallel to the surface.

1.3 Mechanism and Definition of Non-Wettability

The essential characteristic of a non-wettable surface is the ease of removal of a drop from the surface by applying a small force, such as a small fraction of the drop weight. This is usually tested by tilting the surface, similarly to the natural slight tilting of leaves, and measuring the angle at which the drop rolls off. The currently existing quantitative definition, which requires

CA > $\sim 150^\circ$ and roll-off angle < $\sim 5^\circ$, has only an empirical justification. For fundamental understanding and ability to design successful new non-wettable surfaces, it is essential to study this point in more detail. Because of the prevalence of drop-related non-wetting applications, it makes sense to first reach a full understanding of these cases. However, the definition must be made more general. Easy removal of a drop from a solid surface appears to depend on two main factors: (a) the ability of a weak external force to get the drop out of equilibrium, and (b) high rate of removal from the surface. The factor that may keep a drop in equilibrium under the effect of an external force (say, gravity) is contact angle hysteresis, namely the existence of a range of metastable CAs. This allows the drop to assume a non-axisymmetric equilibrium shape as required by the external force. In contrast, on ideal surfaces the drop must be axisymmetric by definition, so it cannot stay in equilibrium even under the influence of a very small force.

Regarding the rate of removal, it is intuitively appealing to assume that the lower is the solid-liquid contact area, the higher is the rate of removal of the liquid from the solid surface.^{12,25,29} If this is true, then the crux of the matter is to find a way to reduce the wetted area as much as possible. The first idea that comes to mind is making the CA as high as possible. However, a simple geometrical calculation indicates that by increasing the Young CA from 90° (considered usually as the lower limit of hydrophobicity) to 120° (the highest available Young CA in practice), the reduction in the area wetted by a drop is only by a factor of about 2. Thus, a different mechanism, capable of much bigger increase in the CA, is required.

Actually, the above two factors that characterize non-wettability can be translated into the following two objectives: (a) achieving a very small hysteresis range (by making the surface as uniform as possible); and (b) making the CA as high as possible. In principle, both objectives can be attained if the surface that is in contact with the liquid consists mostly of a gas, *e.g.* air trapped in roughness grooves. A gas is the most hydrophobic “surface” we can have, and is also the most uniform. Therefore, a CB state, where a liquid is supported by relatively few solid peaks, certainly answers the need. This statement leads to a possible unified definition of all types of non-wettable surfaces. Qualitatively, this definition may simply state that the wetted area has to be sufficiently small. Some initial calculations¹⁴ showed that the wetted area in the CB state may be orders of magnitude lower than that in the W state, even for the same CA. Further quantitative work is required, but it is clear that non-wettability has to be associated with the CB state, as was qualitatively concluded above and also by Quéré.⁸

Whatever the exact definition, from a practical point of view it is clear that in order to be non-wettable the solid surface must be either rough or porous. The grooves of a rough surface are interconnected and open to the atmosphere. In a porous surface, the pores may be either interconnected or isolated. In the latter case it may be much easier to keep the air in the pores in a stable state, but structural constraints may limit the reduction of the wetted area. Therefore, the following discussion is limited only to structures with interconnected grooves or pores.

1.4 Stability Considerations

As previously discussed, roughness of the solid surface is a necessary condition for non-wettability; however, it is not a sufficient condition. As shown below, the geometric characteristics of the roughness may have a major influence. In general, there may be more than one equilibrium position for the liquid–air interface (*i.e.* minima in the Gibbs energy) within the roughness grooves. The most stable is, of course, the one that has the lowest Gibbs energy. Identifying equilibrium positions is easy: the two equilibrium indicators, namely the Young and the Young–Laplace equations, have to be fulfilled. The latter is fulfilled by the curvature of the liquid–gas interface inside the roughness grooves being the same as that of the outer liquid–air interface, as explained above. This is achieved by assuming that this interface is practically flat. Thus, the only question that needs to be considered is whether the local CA can equal the Young CA at the position that is tested. Then, the identified CB states as well as the W state (that is always a potential equilibrium position) have to be compared to find out the most stable state. In the following we discuss first the case of a drop on a solid, non-wettable surface and then that of a non-wettable surface beneath a liquid.

1.4.1 A Drop on a Non-Wettable Surface

To make the above analysis clearer it is best to study some examples. For a drop, it is technically easy to compare energies, since the energy varies monotonically with the apparent CA that the drop makes with the solid surface.^{12,25} Thus, all that is needed in order to decide which state is more stable is to find out which is associated with a lower apparent CA. One of the simplest forms of roughness is that of straight pillars with a square cross-section. Let us assume that the height of the pillars is h , and that they have flat, horizontal tops of width \sqrt{f} that cover an area fraction of f (see Figure 1.1(a)). In this case, there are only two possible equilibrium positions. One is the W state, and the other is the CB state with the liquid–gas interface attached to the top of the pillars. This is so, because it is only at the upper corner of the pillar that the liquid–gas interface can locally attain the Young CA when it is $>90^\circ$ (see Figure 1.1(b)). The roughness ratio is given by

$$r = 1 + 4h\sqrt{f} \quad (1.6)$$

Therefore,

$$\cos\theta_W = r \cos\theta_Y = (1 + 4h\sqrt{f})\cos\theta_Y \quad (1.7)$$

The local roughness ratio of the top of the pillar equals 1, therefore

$$\cos\theta_{CB} = -1 + f(1 + \cos\theta_Y) \quad (1.8)$$

The CB state is more stable if $\theta_{CB} < \theta_W$, namely if $\cos \theta_{CB} > \cos \theta_W$. When $\cos \theta_Y < 0$, this leads to

$$r > 1 + (f - 1)(1 + 1/\cos \theta_Y) \tag{1.9}$$

Thus, for this simple type of roughness, for a given chemistry ($\cos \theta_Y$) and surface density of protrusions (f), the only parameter that determines the stability of the non-wetting state is the roughness ratio that depends on the protrusion height, h . The wetting state turns from W to CB when the roughness ratio, namely height of protrusion, is sufficiently high.

For roughness features that are not flat at the top, the situation is more complex and interesting.^{12,25} A simple example of two-dimensional roughness with a circular cross-section clearly demonstrates the phenomena that may be observed. For convex roughness features (see Figure 1.2(a)) it is

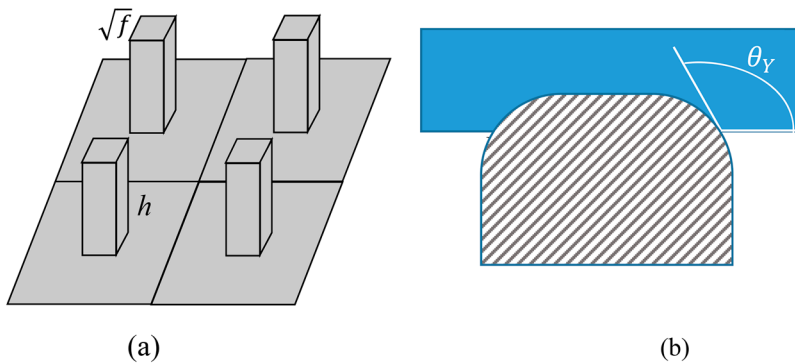


Figure 1.1 (a) A simple form of roughness, for which the transition from the Wenzel regime to the Cassie–Baxter regime depends only on the height of the protrusions, for a given chemistry ($\cos \theta_Y$) and surface density of protrusions (f). (b) The liquid–air interface may find a position that enables the local contact angle (CA) to equal the Young CA at the upper corner of the protrusion.

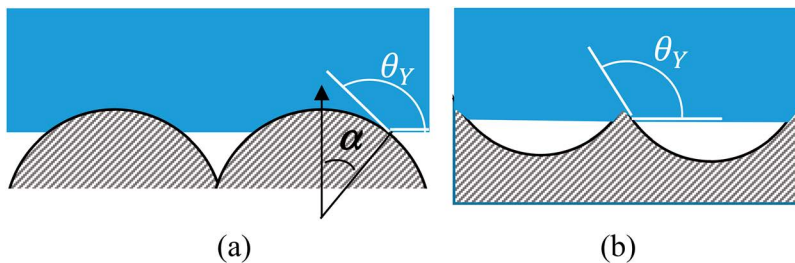


Figure 1.2 Equilibrium position of the liquid inside a roughness groove, as indicated by the contact angle (CA) being equal to the Young CA:¹² (a) convex roughness features; (b) concave roughness features.

possible to get a stable CB state above a certain roughness ratio, as explained in the following. First, a position of the liquid–air interface for which the CA equals the Young CA has to be identified. This is feasible only if the maximum position angle, α , (see Figure 1.2(a)) is bigger than $(180^\circ - \theta_Y)$. Once this condition is fulfilled, we need to check if this position is a minimum in the Gibbs energy. It turns out¹² that indeed it is a minimum, and that above a certain roughness ratio (determined by the maximum value of α) the CB state is more stable than the W state.

The picture is reversed when the roughness features are concave (Figure 1.2(b)). In this case, the Gibbs energy keeps going down as the liquid penetration into the grooves advances until the W state is reached. Thus, although there exists a position where the CA equals the Young CA (Figure 1.2(b)), the system is unstable and must get to the W state. As concluded from additional studies,^{29,43} it turns out that the specific protrusion shape within the group of convex shapes exerts a major effect. Rounded-top protrusions seem to be more effective than flat-topped ones with a sharp edges.^{29,43} This theoretical observation may explain why nature prefers rounded-top protrusions.

The role of fractal or multiscale roughness has attracted attention since the early publications on superhydrophobicity.^{2,15,21,23,28,30,33,34,39} A relatively recent study⁴³ covered a wide range of parameters: three types of roughness geometries with up to four roughness levels (see Figure 1.3). This study showed that the main effect is in reducing the sizes of the roughness protrusions that are necessary for stable superhydrophobicity. Thus, it is not the multiscale nature of the roughness that is responsible for superhydrophobicity; rather, it helps in making the features smaller, therefore more stable from a mechanical point of view.

An interesting extension of the above cases is the one dealing with superhydrophobic surfaces, namely non-wettable surfaces, for which the CAs of the wetting liquid is less than 90° . This case appears at first sight to contradict the common requirement of hydrophobicity for non-wettable surfaces. However, if we look at the CB eqn (1.5), there is no *a priori* reason that prevents $\cos\theta_{CB}$ from being negative, even if $\theta_Y < 90^\circ$. For example, the Young CA may be acute at the equilibrium positions shown in Figure 1.4. However,

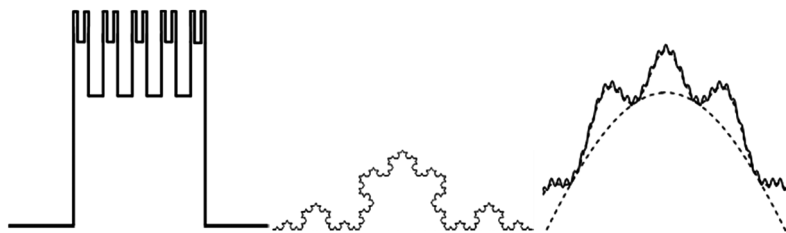


Figure 1.3 Various models of multiscale roughness used in simulations. Reprinted with permission from E. Bittoun and A. Marmur, *Langmuir*, 2012, **28**, 13933. Copyright 2012 American Chemical Society.⁴³

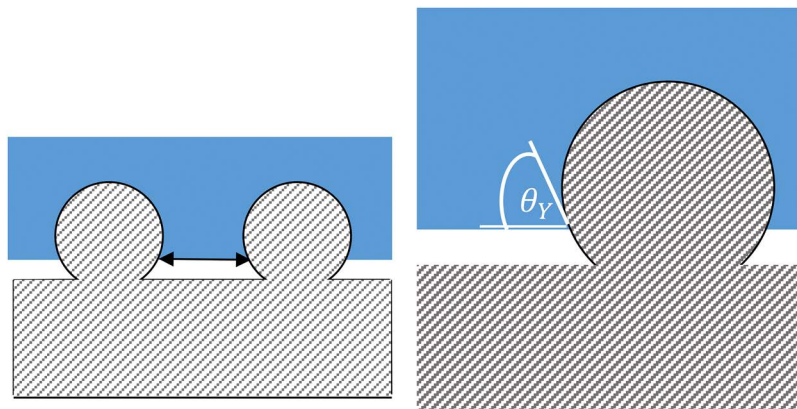


Figure 1.4 Superhydrophobic surface: the liquid–air interface is at equilibrium with a solid rough surface, the Young CA of which is $<90^\circ$.²⁵

stability also needs to be checked for this case. The results of this test lead to conclusions that are similar to those of a drop on a hydrophobic rough surface: it may be stable for convex protrusions, and unstable otherwise.²⁵ Nevertheless, it is important to realize that a superhydrophobic state is necessarily metastable, for the following reason. For a hydrophilic surface, the W state is characterized by a CA that is lower than the Young CA. On the other hand, the whole point in making a super-hydrophobic surface is to increase the CA beyond the Young CA. Thus, the W state, by definition, has a lower CA than the CB state, *i.e.* it is more stable. The special type of roughness that enables superhydrophobicity has been called by several names, such as “multivalued topography” or “re-entrant”.

1.4.2 Underwater Superhydrophobicity

As mentioned in the introduction, there are important reasons for keeping a stable air film on a solid surface under water. This situation is not explicitly defined by apparent CAs related to the W or CB state. However, the concepts of the W and CB states remain valid in terms of the contact between the liquid and the solid.

The equilibrium criteria for the CB state turn out to be the same as for a drop.¹⁸ The local CA between the liquid and the roughness protrusion must be the Young CA, and the curvature of the liquid–air interfaces must appear to be approximately zero, since it equals the curvature of the outside surface of the liquid. The condition that differentiates unstable equilibrium from metastable or stable ones, in terms of the roughness geometry, turns out to be the same as for a drop.¹⁸ The stable CB state in this system is determined by eqn (1.9), which gives a minimum roughness ratio above which the CB state is stable.¹⁸

1.5 Conclusions

The following points summarize the opinion of the author regarding the main fundamentals of non-wetting:

- Non-wettability of solid surfaces may be qualitatively defined by stating that the wetted area must be minimal. This implies that the system must be in the CB state. A quantitative definition of non-wettability is yet to be developed.
- Stable CB states can be achieved by roughness geometry that conforms to a certain mathematical condition.^{12,18,25} For example, convex protrusions enable it while concave cavities do not.
- Non-wetting in systems with an acute Young CA (superhydrophobicity) is feasible, but it is always metastable.
- Multiscale roughness is not essential for non-wettability; however, it improves the mechanical stability of the surface by lowering the required protrusion size.
- The detailed optimal topography of non-wettable surfaces has yet to be elucidated. Moreover, it is likely that there is more than one solution to the problem, depending on specific constraints.

References

1. A. B. D. Cassie and S. Baxter, *Trans. Faraday Soc.*, 1944, **40**, 546.
2. T. Onda, S. Shibuichi, N. Satoh and K. Tsujii, *Langmuir*, 1996, **12**, 2125.
3. C. Neinhuis and W. Barthlott, *Ann. Bot.*, 1997, **79**, 667.
4. S. Herminghaus, *Europhys. Lett.*, 2000, **52**, 165.
5. D. Oner and T. J. McCarthy, *Langmuir*, 2000, **16**, 7777.
6. M. Thieme, R. Frenzel, S. Schmidt, F. Simon, A. Hennig, H. Worch, K. Lunkwitz and D. Scharnweber, *Adv. Eng. Mater.*, 2001, **3**, 691.
7. Z. Yoshimitsu, A. Nakajima, T. Watanabe and K. Hashimoto, *Langmuir*, 2002, **18**, 5818.
8. D. Quéré, *Nat. Mater.*, 2002, **1**, 14.
9. S. Li, H. Li, X. Wang, Y. Song, Y. Liu, L. Jiang and D. Zhu, *J. Phys. Chem. B*, 2002, **106**, 9274.
10. J. Kijlstra, K. Reihls and A. Klamt, *Colloids Surf., A*, 2002, **206**, 521.
11. A. Duparre, M. Flemming, J. Steinert and K. Reihls, *Appl. Opt.*, 2002, **41**, 3294.
12. A. Marmur, *Langmuir*, 2003, **19**, 8343.
13. N. A. Patankar, *Langmuir*, 2003, **19**, 1249.
14. A. Marmur, *Langmuir*, 2004, **20**, 3517.
15. N. A. Patankar, *Langmuir*, 2004, **20**, 8209.
16. A. Otten and S. Herminghaus, *Langmuir*, 2004, **20**, 2405.
17. Y. Cong, G.-h. Chen, Y. Fang and L.-q. Ren, *J. Bionic. Eng.*, 2004, **1**, 249.
18. A. Marmur, *Langmuir*, 2006, **22**, 1400.

19. E. Bormashenko, Y. Bormashenko, T. Stein, G. Whyman and E. Bormashenko, *J. Colloid Interface Sci.*, 2007, **311**, 212.
20. A. Solga, Z. Cerman, B. F. Striffler, M. Spaeth and W. Barthlott, *Bioinspiration Biomimetics*, 2007, **2**, 126.
21. M. Nosonovsky and B. Bhushan, *Ultramicroscopy*, 2007, **107**, 969.
22. F. Peter, *Intrface*, 2007, **4**, 637.
23. Y. Yu, Z.-H. Zhao and Q.-S. Zhengu, *Langmuir*, 2007, **23**, 8212.
24. J. Genzer and A. Marmur, *MRS Bull.*, 2008, **33**, 742.
25. A. Marmur, *Langmuir*, 2008, **24**, 7573.
26. A. Tuteja, W. Choi and J. M. Mabry, *et al.*, *Proc. Natl. Acad. Sci. U. S. A.*, 2008, **105**, 18200.
27. D. Quéré, *Annu. Rev. Mater. Res.*, 2008, **38**, 71.
28. W. Li and A. Amirfazli, *Soft Matter*, 2008, **4**, 462.
29. E. Bittoun and A. Marmur, *J. Adhes. Sci. Technol.*, 2009, **23**, 401.
30. K. Koch, H. F. Bohn and W. Barthlott, *Langmuir*, 2009, **25**, 14116.
31. N. J. Shirtcliffe, G. McHale and M. I. Newton, *Langmuir*, 2009, **25**, 14121.
32. Y. Su, B. Ji, K. Zhang, H. Gao, Y. Huang and K. Hwang, *Langmuir*, 2010, **26**, 4984.
33. S. H. Sajadinia and F. Sharif, *J. Colloid Interface Sci.*, 2010, **344**, 575.
34. T. Liu, W. Sun, X. Sun and H. Ai, *Langmuir*, 2010, **26**, 14835.
35. W. Barthlott, T. Schimmel and S. Wiersch, *et al.*, *Adv. Mater.*, 2010, **22**, 2325.
36. G. McHale, M. I. Newton and N. J. Shirtcliffe, *Soft Matter*, 2010, **6**, 714.
37. Y. Su, B. Ji, K. Zhang, H. Gao, Y. Huang and K. Hwang, *Langmuir*, 2010, **26**, 4984.
38. S. H. Sajadinia and F. Sharif, *J. Colloid Interface Sci.*, 2010, **344**, 575.
39. H. H. Liu, H. Y. Zhang and W. Li, *Langmuir*, 2011, **27**, 6250.
40. C. W. Extrand, *Langmuir*, 2011, **27**, 6920.
41. S.-H. Hsu, K. Woan and W. Sigmund, *Mater. Sci. Eng., R*, 2011, **72**, 189.
42. A. Marmur, *Soft Matter*, 2012, **8**, 6867.
43. E. Bittoun and A. Marmur, *Langmuir*, 2012, **28**, 13933.
44. N. R. Geraldi, F. F. Ouali and R. H. Morris, *et al.*, *Appl. Phys. Lett.*, 2013, **102**, 214104.
45. P. R. Jones, X. Hao and E. R. Cruz-Chu, *et al.*, *Sci. Rep.*, 2015, **5**, 12311.
46. R. Ramachandran and M. Nosonovsky, *Phys. Chem. Chem. Phys.*, 2015, **17**, 24988.
47. G. Wolansky and A. Marmur, *Langmuir*, 1998, **14**, 5292.
48. R. N. Wenzel, *J. Ind. Eng. Chem.*, 1936, **28**, 988.
49. A. Marmur and E. Bittoun, *Langmuir*, 2009, **25**, 1277.
50. B. Haimov, S. Pechook, O. Ternyak and B. Pokroy, *J. Phys. Chem. C*, 2013, **117**, 6658.

Non-Wetting, Stabilization, and Phase Transitions Induced by Vibrations and Spatial Patterns

RAHUL RAMACHANDRAN^a AND MICHAEL NOSONOVSKY*^a

^aUniversity of Wisconsin-Milwaukee, 3200 N Cramer St, Milwaukee, WI 53211, USA

*E-mail: nosonovs@uwm.edu

2.1 Introduction

Small fast vibrations constitute a temporal periodic pattern, while surface microtopography often introduces spatial patterns. Despite the fact that both types of patterns are small, they can significantly affect and alter the bulk properties of materials. We show in this chapter how small fast vibrations can be substituted by an effective force, which stabilizes an inverted pendulum or bouncing droplets. We call this effective force a “levitation” force, given that it provides support to suspended objects, such as liquid droplets, due to the effect of the vibro-levitation.

Levitation is the process by which an object is suspended by a physical force against gravity. Historically, levitation was claimed by many ancient spiritual or occult teachings, but the possibility of levitation as a physical phenomenon was also studied by many scholars including Isaac Newton, who secretly

investigated the possibility of levitation as an opposite force to gravitation.^{1,2} Today physicists investigate several means of levitation including magnetic, electrostatic, acoustic, and aerodynamic forces.³ Acoustic levitation is one interesting possibility. The phenomenon is based on the non-linear nature of intense sound waves resulting in the acoustic radiation pressure creating an average positive force on a suspended object which resists the weight of the object.

Of particular interest is the acoustic levitation of a small droplet. Droplets, despite their apparent simplicity, are quite complex objects involving such effects as surface tension, Laplace pressure, capillary waves, and non-linear viscosity.⁴⁻¹¹ Droplet transport, coalescence, and bouncing off solid and liquid surfaces is still not completely understood, since these processes involve complex interactions and lead to complicated scenarios of droplet evolution. This complexity of droplet behaviour makes droplets suitable for various applications. In the past, it has been suggested that the droplets could be used for microfluidic applications; for instance, they could serve as microreactors for various chemical compounds carried by coalescent water droplets. For example, it has been shown that droplet coalescence can realize Boolean logic and thus a “droplet computer” can in principle be created.¹²

Recent studies have shown experimentally that incoming droplets can bounce off a vibrating liquid surface, thus leading to the “walking droplets”, which, in a sense, combine the properties of waves and particles and serve as an illustration of the particle-wave duality.^{13,14} The effect of bouncing droplets is thought to be similar to the acoustic levitation due to non-linear viscosity in a thin film. However, a detailed model of such an effect remains quite complex, and several ideas have been suggested in the literature.

It has been suggested¹⁵ that the classical stability problem of an inverted pendulum on a vibrating foundation has relevance to a diverse class of non-linear effects involving dynamic stabilization of statically unstable systems ranging from the vibrational stabilization of beams to novel “dynamic materials,” the transport and separation of granular material, soft matter, bubbles and droplets, to synchronization of rotating machinery. In these problems, the small fast vibrational motion can be excluded from consideration and substituted by effective slow forces acting on the system causing the stabilizing effect.¹⁶

In this chapter we suggest a simple analogy between levitating droplets over a vibrating liquid surface and a well-known mechanical system consisting of an inverted pendulum on a vibrating foundation. This analogy sheds light on the necessary conditions for droplet levitation. We further discuss the relation of the phenomenon to other non-linear vibration-caused effects, such as the vibro-levitation of a flexible stiff rope (“Indian rope trick”), the shear-thickening of non-Newtonian fluids (“cornstarch monsters”), and vibration-induced phase transitions, as well as possible applications for “smart” dynamic nanocomposite materials.¹⁷

2.2 Effective Force Corresponding to Small Fast Vibrations

In this section, we study pure mechanical systems undergoing fast vibrations in a time-independent potential field. Two different approaches have been developed to separate the fast small vibrations from the overall motion of the system; the Mathieu equation approach and Kapitza's method of the separation of motions. The latter method was further developed by Blekhman who suggested an interesting interpretation with two observers. One observer can see the small vibrations while the other one, who does not see the vibrations (*e.g.* due to a specially designed stroboscopic light), nonetheless observes their effect as a fictitious force, similar to the force of inertia. We will discuss various examples and derive a mathematical expression for an effective stabilizing “vibro-levitation” force. First we discuss a general case of Kapitza's separation of fast and slow motions. Kapitza thought of such systems being in a state of slow oscillation with a fast vibration superimposed upon it. The effect of fast vibrations can be isolated as a change in the effective potential energy of the system. Following Blekhman, an observer in a vibrating frame of reference will perceive the stability as a result of an additional fictitious force, which we refer to as the vibro-levitation force. We apply this method to the classic example of an inverted pendulum, and calculate the vibro-levitation force. This is followed by a review of the Mathieu equation approach to studying the stability of an inverted pendulum. Then, we look at the stabilization of multiple pendulums, and a continuous system involving a rope. Replacing fast vibrations with an effective force can not only be applied to systems described above, but also to non-coalescing droplets on a vibrating bath and other liquid systems which are discussed in later sections.

2.2.1 Motion Subjected to a Rapidly Oscillating Force

The method of separation of motions was first suggested by Kapitza¹⁶ to study the stability of a pendulum on a vibrating foundation and then generalized for the case of an arbitrary motion in a rapidly oscillating field by Landau and Lifshitz.¹⁸

Consider a material point with mass m in a potential field $\Pi(x)$, where x is a spatial coordinate, with the minimum corresponding to the stable equilibrium. One can think about a mechanical spring-mass system as shown in Figure 2.1a. The restoring “spring force” acting on the mass is given by $-d\Pi/dx$, therefore, the equation of motion of the system is $m\ddot{x} = -d\Pi/dx$. In addition to the time-independent potential field $\Pi(x)$, a “fast” external periodic force $f\cos\Omega t$ acts upon the mass with a small-amplitude f and high

frequency $\Omega \gg \sqrt{(d^2\Pi/dx^2)/m}$, which is much higher than the natural frequency (Figure 2.1b). The equation of motion then becomes

$$m\ddot{x} = -(d\Pi/dx) + f\cos\Omega t \quad (2.1)$$

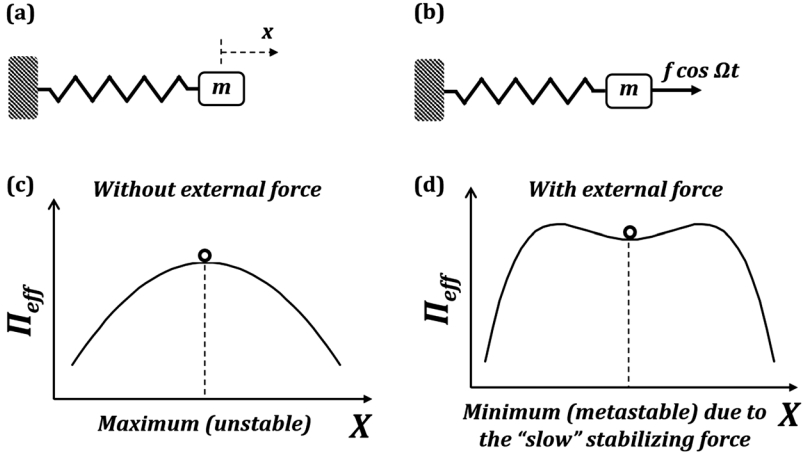


Figure 2.1 (a) Motion in one dimension of a mass m connected to a spring. (b) Application of an external force $f \cos \Omega t$ to the mass m . (c) Unstable equilibrium corresponding to the maximum potential energy. (d) A metastable equilibrium due to the stabilizing effect of the external force.

The location of the mass can be written as a sum of the “slow” oscillations $X(t)$ due to the “slow” force and small “fast” oscillations $\zeta(t)$ due to the “fast” force:

$$x(t) = X(t) + \zeta(t) \quad (2.2)$$

The mean value $\bar{\zeta}(t)$ of this fast oscillation over its period $2\pi/\Omega$ is zero, whereas $X(t)$ changes slightly during the same period:

$$\bar{\zeta}(t) = \frac{\Omega}{2\pi} \int_0^{2\pi/\Omega} \zeta(t) dt = 0 \quad (2.3)$$

$$\bar{X}(t) \approx X(t) \quad (2.4)$$

Therefore the mean location of the mass can be written as

$$\bar{x}(t) = \bar{X}(t) + \bar{\zeta}(t) \approx X(t) \quad (2.5)$$

and the second derivative as

$$\ddot{\bar{x}}(t) \approx \ddot{X}(t) \quad (2.6)$$

Substituting eqn (2.2) in eqn (2.1) and using the Taylor series first-order terms in powers of ζ ,

$$m\ddot{X} + m\ddot{\zeta} = -\frac{d\Pi}{dx} - \zeta \frac{d^2\Pi}{dx^2} + f \cos \Omega t + \zeta \frac{\partial(f \cos \Omega t)}{\partial X} \quad (2.7)$$

The “slow” and “fast” terms in eqn (2.7) must separately be equal. The second derivative of small “fast” oscillations ζ is proportional to Ω^2 which is a large term. The terms on the right-hand side of eqn (2.7) containing the small ζ are neglected. This gives $m\ddot{\zeta} = f \cos \Omega t$, and integrating with respect to time t ,

$$\xi = -\frac{f \cos \Omega t}{m\Omega^2} \quad (2.8)$$

Averaging eqn (2.7) with respect to time, substituting the relation $\frac{\Omega}{2\pi} \int_0^{2\pi/\Omega} f \cos \Omega t dt = 0$, eqn (2.3)–(2.6), and eqn (2.8) gives

$$m\ddot{X} = -\frac{d\Pi}{dX} + \overline{\xi \frac{\partial(f \cos \Omega t)}{\partial X}} = -\frac{d\Pi}{dX} - \frac{1}{m\Omega^2} \overline{f \cos \Omega t \frac{\partial(f \cos \Omega t)}{\partial X}}$$

$$m\ddot{X} = -\frac{d\Pi}{dX} - \frac{1}{2m\Omega^2} \overline{\frac{\partial(f \cos \Omega t)^2}{\partial X}} \quad (2.9)$$

This can be written as $m\ddot{X} = -\frac{d\Pi_{\text{eff}}}{dX}$ where Π_{eff} is an effective potential energy given by

$$\Pi_{\text{eff}} = \Pi + \overline{\frac{(f \cos \Omega t)^2}{2m\Omega^2}} = \Pi + \frac{f^2}{4m\Omega^2} = \Pi + \frac{m}{2} \bar{\xi}^2 \quad (2.10)$$

Thus the effect of “fast” vibrations ζ when averaged over the time period $2\pi/\Omega$ is equivalent to the additional term $m\bar{\xi}^2/2$ on the right-hand side in eqn (2.10). This term is the mean kinetic energy of the system under “fast” oscillations. Thus small “fast” vibrations can be substituted by an additional term in the potential energy resulting in the same effect that oscillations have on the system. The most interesting case is when this term affects the state of the equilibrium of a system. Let us say that in the absence of vibrations a system has an effective potential energy $\Pi_{\text{eff}} = \Pi$ (a local maximum of the potential energy, Figure 2.1c). Vibrations can bring this system to a stable equilibrium due to the additional term discussed before (a local minimum of the potential energy, Figure 2.1d). In such cases the small “fast” vibrations have a stabilizing effect on the state of equilibrium.

Blekhman¹⁵ has applied the method of separation of motions to many mechanical systems and suggested what he called “vibrational mechanics” as a tool to describe a diverse range of effects in the mechanics of solid and liquid media, from effective liquefying of granular media, which can flow through a hole like a liquid when on a vibrating foundation, to the opposite effect of solidifying liquid by jamming a hole in a vessel on a vibrating

foundation, to vibro-synchronization of the phase of two rotating shafts on a vibrating foundation.

Blekhman¹⁵ has also suggested an elegant interpretation of the separation of motions. According to his interpretation, there are two different observers who can look at the vibrating system. One is an ordinary observer in an inertial frame of reference who can see both small, ζ , and large, X , oscillations. The other one is a “special” observer in a vibrating frame of reference, who does not see the small-scale motion, ζ , possibly due to a stroboscopic effect or just because his vision is not sensitive enough to see the small-scale motion. As a result, what the ordinary observer sees as an effect of the fast small vibrations is perceived by the special observer as an effect of some new effective force. This fictitious force is similar to the inertia force which is observed by observers in a non-inertial frame of reference. Furthermore, when the stabilizing effect occurs, the special observer attributes the change in effective potential energy to fictitious “slow” stabilizing forces or moments. The additional “slow” stabilizing force V for the system can be written as

$$V = -\frac{\partial}{\partial X} \left(\frac{f^2}{4m\Omega^2} \right) \quad (2.11)$$

The most common example of the stabilizing effect of the small vibrations is the inverted pendulum, which is studied in the following section.

2.2.2 Inverted Pendulum

We now consider the classic problem of stability of an inverted pendulum to apply the method of the separation of motions and determine a stabilizing vibro-levitation force. A simple pendulum is a common example used in mechanics to introduce the fundamentals of simple harmonic motion. Consider a pendulum with a point mass m connected to the end of a pivoted link of length L . The angular position of the pendulum about its pivot is described by the angle ψ . It has its stable equilibrium at its vertical lower position, $\psi = 0^\circ$ where the potential energy is minimum as shown in Figure 2.2. Any small perturbations from this position results in oscillations about the equilibrium with natural frequency $\omega = \sqrt{g/L}$ where g is the acceleration due to gravity. Eventually the pendulum returns to its equilibrium due to the restoring force $-\frac{d(mgL \cos \psi)}{d\psi}$.

A pendulum also has an unstable equilibrium that corresponds to the point of inflection at $\psi = 180^\circ$ (Figure 2.2). When the foundation of the pendulum is subjected to vertical harmonic oscillations $A \cos \Omega t$, where A is the amplitude and $\Omega \gg \omega$ is the frequency, the equilibrium at $\psi = 180^\circ$ can, under certain conditions, become stable. A pendulum on a vibrating foundation is called “Kapitza’s pendulum” after Peter Kapitza. The equation of motion can be written as

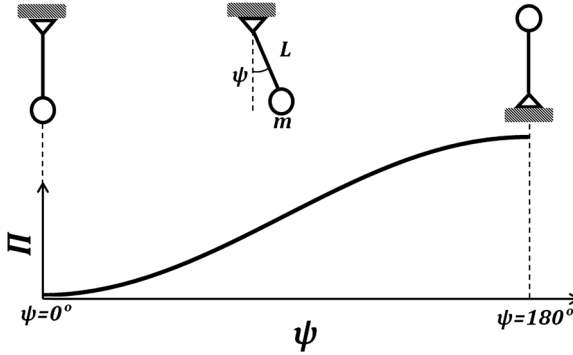


Figure 2.2 The potential energy Π of a pendulum as a function of its angular displacement ψ .

$$L\ddot{\psi} = g \sin \psi - A\Omega^2 \sin \psi \cos \Omega t \quad (2.12)$$

The form of eqn (2.12) is similar to that of eqn (2.1) with $f = -mA\Omega^2 \sin \psi$. Substituting f into eqn (2.10), the effective potential energy can be obtained as

$$\Pi_{\text{eff}} = mgL \left(-\cos \psi + \frac{A^2 \Omega^2}{4gL} \sin^2 \psi \right) \quad (2.13)$$

Now if we look at the stabilized inverted pendulum, it appears upright and stationary. By differentiating the effective potential energy in eqn (2.13) we obtain the generalized force (with the dimension of torque) acting upon the pendulum. In addition to the term involving $\sin \psi$, this generalized force now involves the term given by eqn (2.11):

$$V = \frac{\partial}{\partial \psi} \left(-\frac{mA^2 \Omega^2}{4} \sin^2 \psi \right) = -\frac{mA^2 \Omega^2}{4} \sin 2\psi \quad (2.14)$$

Note that V is dimensionally a torque, because the spatial coordinate ψ is angular displacement. This additional effective force can have a stabilizing effect on the unstable equilibrium. The effect of this force is equivalent to that of a spring with spring constant $k = \frac{mA^2 \Omega^2}{2}$ when the angle ψ is close to 180° . This is equivalent to the upright pendulum supported by a spring (Figure 2.3).

The equilibrium is stable when the effective potential energy in eqn (2.13) is a positive-definite function near the state of equilibrium, which yields the stability criterion

$$A^2 \Omega^2 > 2gL \quad (2.15)$$

Thus, when the amplitude and frequency of the small fast vibrations of the foundation satisfy eqn (2.15), the otherwise unstable equilibrium at

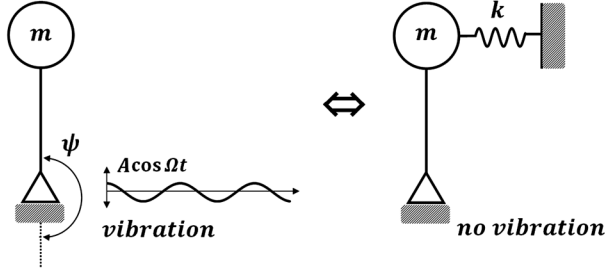


Figure 2.3 The figure on the left shows an inverted pendulum stabilized by a foundation vibrating with a periodic displacement $A \cos \Omega t$. The same system can be represented as shown in the figure on the right with the pendulum being stabilized by a spring of effective spring constant k . Reproduced from ref. 11 with permission from the Royal Society of Chemistry.

$\psi = 180^\circ$ can correspond to a local minimum for the effective potential energy, *i.e.* it can become a stable equilibrium. Thus, we have derived the expression for the stabilizing force (eqn (2.14)) and a stability criterion for the inverted pendulum (eqn (2.15)) using the separation of motion method. We will apply this method to study non-coalescing liquid droplets later in this chapter.

2.2.3 Mathieu Equation Method

The result in eqn (2.15) has been historically obtained using a different method, namely, the parametric resonance Mathieu equation analysis suggested by A. Stephenson in 1908.^{19,20} The motion of a pendulum on a vibrating foundation is an example of parametric oscillation. The differential equation of motion of such a pendulum contains time-varying coefficients and is called the Mathieu equation. Stephenson found that when the pivot of a pendulum is subjected to a vertical periodic motion at a frequency $2\omega/n$ where n is any integer, then the oscillations of the pendulum are gradually amplified. The pendulum eventually becomes highly unstable. Stephenson used the Mathieu equation approach to study the conditions for stability and instability of the pendulum. In this section we briefly describe the Mathieu equation approach to determining the stability criteria of an inverted pendulum.

The equation of motion of a pendulum on a vibrating foundation (eqn (2.12)) can be rewritten as

$$\ddot{\psi} - \left(\frac{g}{L} - \frac{A\Omega^2}{L} \cos \Omega t \right) \sin \psi = 0 \quad (2.16)$$

which has the form of the Mathieu equation. To study the stability of a solution of eqn (2.16) using the perturbation technique, the variables $z = \psi$, $\delta = 4g/L\Omega^2$, $\varepsilon = 2A/L$, where $\varepsilon \ll 1$ and $\tau = \Omega t$, are introduced. For small values of z , $\sin z \approx z$ and the equation of motion for a pendulum reduces to

$$\ddot{z} - \frac{\Omega^2}{4} (\delta - 2\varepsilon \cos \tau) z = 0 \quad (2.17)$$

The stability of a pendulum with vibrating foundation is studied in the parameter plane (δ, ϵ) , with regions of stability and instability, the graphical representation of which is called the Ince–Strutt diagram. For an inverted pendulum the stability criterion is

$$-\frac{1}{2}\epsilon^2 + \frac{7}{8}\epsilon^4 \dots < \delta < 1 - \epsilon - \frac{1}{8}\epsilon^2 \dots \tag{2.18}$$

and is represented by the shaded region in Figure 2.4. For stability at any δ , there is an upper and lower bound for ϵ . It follows that for a certain length of the inverted pendulum there exists a stability range of frequencies $\Omega_1 < \Omega < \Omega_2$. From eqn (2.18), the stability criterion can be obtained as follows. Since we are concerned with an inverted pendulum, we restrict ourselves to the set of negative values of δ in the vicinity of zero and we can write

$$-\frac{1}{2}\epsilon^2 < -\delta \tag{2.19}$$

Substituting $\delta = 4g/L\Omega^2$ and $\epsilon = 2A/L$ into eqn (2.19) we obtain the same stability criteria as in eqn (2.15). The Mathieu equation approach is another way of analysing the vibro-levitation of an inverted pendulum.

We see that the Mathieu equation approach provides the same stability criterion as the method of separation of motion. However, the latter has a more general application and is not limited to the parametric excitation of a pendulum. We can therefore apply the method of separation of motion to more complex problems of the multiple pendulum, the continuous (flexible stiff beam) pendulum, and liquid systems like non-coalescing droplets. We also draw an analogy between mechanical systems undergoing vibration and non-linear behaviour in vibrating fluids that leads to non-wetting and phase transition.

2.2.4 Multiple Pendulums and the Indian Rope Trick

We have discussed the stabilization of a single inverted pendulum by small-amplitude fast vibration of the pendulum’s foundation. Inverted multiple pendulums consisting of a number of freely jointed links can also be stabilized by applying a harmonic oscillation at the foundation as long as the frequency of the oscillation is sufficiently large. The theoretical proof was put

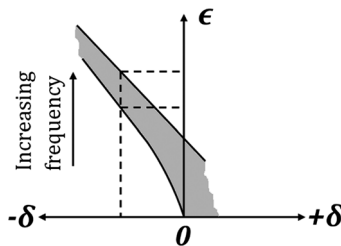


Figure 2.4 The region of stability for an inverted pendulum as seen in the Ince–Strutt diagram. Adapted from ref. 11 with permission from the Royal Society of Chemistry.

forward by Stephenson²¹ who derived the stability criteria. Acheson derived the stability criterion for a multiple pendulum using the Mathieu equation approach. He showed that the region of stability in the Ince–Strutt diagram diminishes as the number of links in the pendulum increases. As the number of links approaches infinity, as in the case of a perfectly flexible string, the region of stability vanishes.²² Acheson and Mullin later experimentally demonstrated the stability of double and triple inverted pendulums.²³

An even more complex, albeit related, case is a continuous system consisting of a flexible beam. Since it has been shown that the limiting case of multiple pendulums, *i.e.* a string, cannot be stabilized in the upside-down position, flexural stiffness must be introduced.

Interestingly, some researchers have suggested that stabilization by a vibrating foundation can explain the so-called Indian rope trick. This trick involves a magician (traditionally an Indian fakir) throwing one end of a flexible rope vertically upwards, which under certain conditions levitates like a vertical rod. In certain versions of the trick a small animal (an ape) could even climb the rope, leaving the audience in awe. This defies the empirical observation that an upright column exceeding a critical length will buckle under its own weight. Although accounts of the trick remain controversial, it has been shown that a rope with bending stiffness can be stabilized at sufficiently high frequencies. A piece of steel curtain wire longer than its critical buckling length was able to stay upright when its pivot was vibrated within a certain frequency range $\Omega_1 < \Omega < \Omega_2$. When the frequencies were reduced below Ω_1 the wire fell over, while increasing the frequencies above Ω_2 resulted in instabilities in the wire.²⁴ Ramachandran and Nosonovsky¹¹ demonstrated instabilities in a plastic rope when its pivot was oscillated at a certain range of frequencies. The rope, which was initially in a buckled state, became unstable at a certain frequency (Figure 2.5). The instabilities grew with increase in frequency till an upper limit

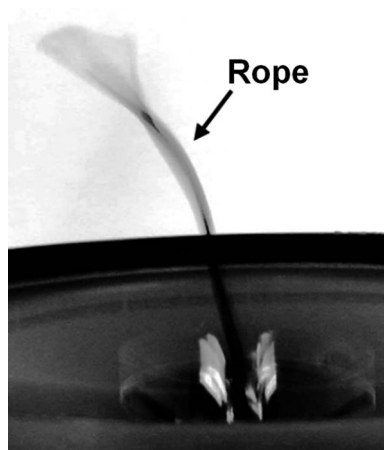


Figure 2.5 Instabilities in a plastic rope on a foundation vibrating at 130 Hz. Reproduced from ref. 11 with permission from the Royal Society of Chemistry.

was reached, beyond which the instabilities gradually decreased and the rope returned to its buckled state.

Now we derive the expression for the stabilizing force for multiple pendulums and a flexible stiff rope. First let us consider a double pendulum as shown in Figure 2.6 with point masses m_1 and m_2 attached to links of lengths L_1 and L_2 respectively. The foundation of the pendulum is subjected to a harmonic oscillation $A \cos \Omega t$. Let the angular displacements of masses m_1 and m_2 be ψ_1 and ψ_2 respectively.

For m_1 we can write the horizontal and vertical displacements as $x_1 = L_1 \sin \psi_1$ and

$y_1 = L_1 \cos \psi_1 + A \cos \Omega t$. Similarly for m_2 , $x_2 = L_1 \sin \psi_1 + L_2 \sin \psi_2$ and

$y_2 = L_1 \cos \psi_1 + L_2 \cos \psi_2 + A \cos \Omega t$. The x and y components of velocities are

$$\dot{x}_1 = L_1 \dot{\psi}_1 \cos \psi_1,$$

$$\dot{y}_1 = -L_1 \dot{\psi}_1 \sin \psi_1 - A \Omega \sin \Omega t, \quad \dot{x}_2 = L_1 \dot{\psi}_1 \cos \psi_1 + L_2 \dot{\psi}_2 \cos \psi_2 \text{ and}$$

$$\dot{y}_2 = -L_1 \dot{\psi}_1 \sin \psi_1 - L_2 \dot{\psi}_2 \sin \psi_2 - A \Omega \sin \Omega t.$$

The kinetic energy of the system is given by $K = \frac{1}{2} m_1 (\dot{x}_1^2 + \dot{y}_1^2) + \frac{1}{2} m_2 (\dot{x}_2^2 + \dot{y}_2^2)$.

The potential energy of the system is given by $\Pi = m_1 g y_1 + m_2 g y_2$. The Lagrangian of the system can be written in terms of the angular displacements and their derivatives as $L = K - \Pi$:

$$\begin{aligned} L = & \frac{1}{2} m_1 (L_1^2 \dot{\psi}_1^2 + A^2 \Omega^2 \sin^2 \Omega t + 2L_1 \dot{\psi}_1 A \Omega \sin \psi_1 \sin \Omega t) \\ & + \frac{1}{2} m_2 \left(L_1^2 \dot{\psi}_1^2 + L_2^2 \dot{\psi}_2^2 + 2L_1 L_2 \dot{\psi}_1 \dot{\psi}_2 \cos(\psi_1 - \psi_2) \right. \\ & \left. + 2A \Omega \sin \Omega t (L_1 \dot{\psi}_1 \sin \psi_1 + L_2 \dot{\psi}_2 \sin \psi_2) + A^2 \Omega^2 \sin^2 \Omega t \right) \\ & - m_1 g (L_1 \cos \psi_1 + A \cos \Omega t) - m_2 g (L_1 \cos \psi_1 + L_2 \cos \psi_2 + A \cos \Omega t) \end{aligned} \quad (2.20)$$

The equations of motion are then given by the Lagrange equations

$$\frac{d}{dt} \left(\frac{\partial L}{\partial \dot{\psi}_1} \right) - \frac{\partial L}{\partial \psi_1} = 0 \text{ and } \frac{d}{dt} \left(\frac{\partial L}{\partial \dot{\psi}_2} \right) - \frac{\partial L}{\partial \psi_2} = 0 \quad (2.21)$$

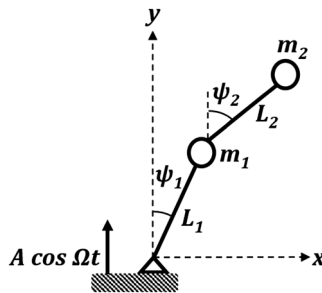


Figure 2.6 An inverted double pendulum whose foundation is subjected to a sinusoidal vibration $A \cos \Omega t$.

Substituting for L and simplifying we obtain

$$(m_1 + m_2)L_1\ddot{\psi}_1 + m_2L_2\ddot{\psi}_2 \cos(\psi_1 - \psi_2) + m_2L_2\dot{\psi}_2^2 \sin(\psi_1 - \psi_2) - m_1gL_1 \sin\psi_1 - m_2gL_1 \sin\psi_1 + A\Omega^2 \cos\Omega t(m_1 \sin\psi_1 + m_2 \sin\psi_1) = 0$$

and

$$m_2L_2\ddot{\psi}_2 + m_2L_1\ddot{\psi}_1 \cos(\psi_1 - \psi_2) - m_2L_1\dot{\psi}_1^2 \sin(\psi_1 - \psi_2) - m_2gL_2 \sin\psi_2 + m_2A\Omega^2 \sin\psi_2 \cos\Omega t = 0$$

Rewriting the equations of motion in the form of eqn (2.1), we have

$$(m_1 + m_2)L_1\ddot{\psi}_1 + m_2L_2\ddot{\psi}_2 \cos(\psi_1 - \psi_2) + m_2L_2\dot{\psi}_2^2 \sin(\psi_1 - \psi_2) = m_1gL_1 \sin\psi_1 + m_2gL_1 \sin\psi_1 - (m_1 + m_2)A\Omega^2 \sin\psi_1 \cos\Omega t$$

and

$$m_2L_2\ddot{\psi}_2 + m_2L_1\ddot{\psi}_1 \cos(\psi_1 - \psi_2) - m_2L_1\dot{\psi}_1^2 \sin(\psi_1 - \psi_2) = m_2gL_2 \sin\psi_2 - m_2A\Omega^2 \sin\psi_2 \cos\Omega t$$

Comparing these with eqn (2.1), we see

$$f_1 = -(m_1 + m_2)A\Omega^2 \sin\psi_1 \text{ and } f_1 = -m_2A\Omega^2 \sin\psi_2 \quad (2.22)$$

Using eqn (2.11), the effective generalized forces on m_1 and m_2 can be written as

$$V_1 = \frac{\partial}{\partial\psi_1} \left(\frac{f_1^2}{4m_1\Omega^2} \right) = -\frac{(m_1 + m_2)^2}{4m_1} A^2 \Omega^2 \sin 2\psi_1$$

$$V_2 = \frac{\partial}{\partial\psi_2} \left(\frac{f_2^2}{4m_2\Omega^2} \right) = -\frac{m_2}{4} A^2 \Omega^2 \sin 2\psi_2 \quad (2.23)$$

For any mass m_i in a system of n connected pendulums as shown in Figure 2.7,

$$f_i = -A\Omega^2 \left(\sum_{j=i}^n m_j \right) \sin\psi_i \quad (2.24)$$

and the stabilizing effective generalized force is

$$V_i = \frac{\partial}{\partial\psi_i} \left(\frac{f_i^2}{4m_i\Omega^2} \right) = -\frac{A^2\Omega^2}{4m_i} \left(\sum_{j=i}^n m_j \right)^2 \sin 2\psi_i \quad (2.25)$$

The multiple pendulums are stabilized due to the system of effective generalized forces $\{V_1, V_2, \dots, V_n\}$ as shown in Figure 2.7. For small angular

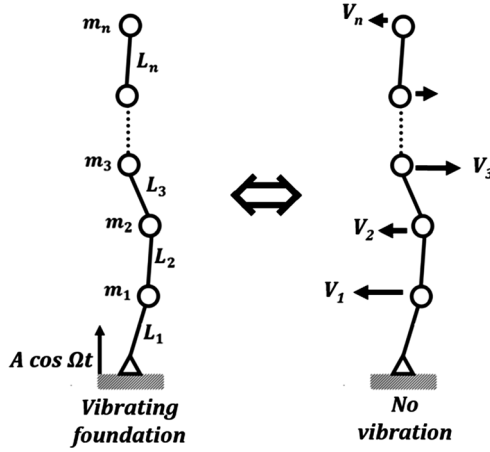


Figure 2.7 A multiple pendulum which is being stabilized by vibrating its foundation is equivalent to a multiple pendulum which is stabilized by a system of generalized vbro-levitation forces V_1, V_2, \dots, V_n .

displacements of the system of n connected pendulums, the equivalent spring constant at the first link is

$$k_1 = \frac{A^2 \Omega^2}{2m_1} \left(\sum_{i=1}^n m_i \right)^2 \tag{2.26}$$

Studies of the Indian rope trick usually approximate the rope or wire to continuum objects such as a rod or column with appreciable stiffness. For example, Champneys and Fraser²⁵ studied the Indian rope trick for a linearly elastic rod. The equation of motion in terms of the lateral displacement u at arc length s is

$$\eta \frac{\partial^2 u}{\partial t^2} + (1 - \eta \varepsilon \cos t) \frac{\partial}{\partial s} \left((1 - s) \frac{\partial u}{\partial s} \right) + b \frac{\partial^4 u}{\partial s^4} = 0 \tag{2.27}$$

where η, ε , and b are the dimensionless acceleration, amplitude, and stiffness respectively. Comparing this with eqn (2.1) we can write

$$f = \eta \varepsilon \frac{\partial}{\partial s} \left((1 - s) \frac{\partial u}{\partial s} \right)$$

and formulate the effective vbro-levitation force using eqn (2.11).

Shishkina *et al.* investigated a rope treated as a flexible Euler beam with the stiffness k subjected to the gravity and an axial load oscillating near the constant value of c^2 with amplitude εa^2 and frequency Ω . The transversal deflection of the beam $u(x,t)$ is governed by

$$\frac{\partial^2 u}{\partial t^2} + k \frac{\partial^4 u}{\partial x^4} + (c^2 + \varepsilon \Omega^2 \sin \Omega t) \frac{\partial u}{\partial x} + (c^2 + \varepsilon \Omega^2 \sin \Omega t) x \frac{\partial^2 u}{\partial x^2} = 0 \tag{2.28}$$

They showed that effect of the oscillating load is equivalent to the increase of the effective flexural stiffness of the rope k , which becomes equal to

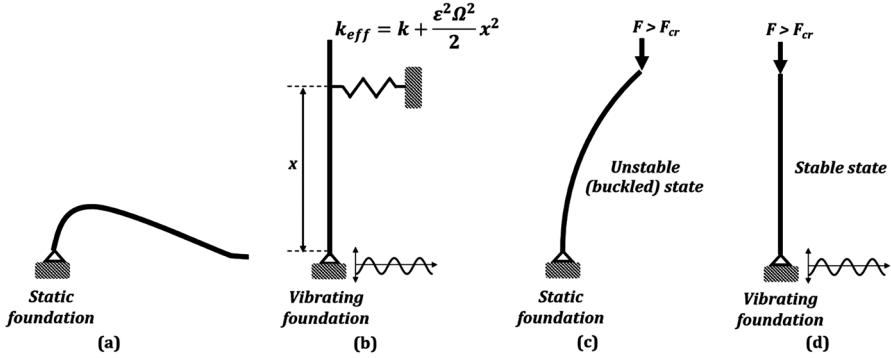


Figure 2.8 (a) A rope which is subject to no vibration buckles under its own weight. (b) Vertical vibrations results in an increased effective stiffness which prevents buckling. (c) For any beam there is a critical force (F_{cr}) that depends on the beam material and geometry. Any load (F) greater than this will cause the beam to buckle. (d) Vibrating the foundation leads to an increase in the effective stiffness of the beam, and the beam is able to resist buckling.

$k_{\text{eff}} = k + \frac{\epsilon^2 \Omega^2}{2} x^2$, where x is the distance along the rope (Figure 2.8a and b). This increase can be sufficient to exceed the critical value of the stiffness and prevent buckling of the beam (Figure 2.8c and d).²⁶

For a multiple pendulum of n connected links, as $n \rightarrow \infty$ the system becomes more flexible and its stiffness decreases. Now the system is similar to a limp rope. From eqn (2.25), the vibro-levitation force is proportional to the mass. Therefore as $n \rightarrow \infty$, the vibro-levitation force becomes infinite. It follows that the Indian rope trick cannot be performed if the rope does not have sufficient inherent stiffness.

In the previous sections we introduced the method of separation of motions, applied it to various mechanical systems undergoing vibration, and derived an effective stabilizing force for each case. In the next section, we study non-coalescing droplets stabilized by vibrations. We also apply the method of separation of motions to formulate an expression for the effective force that causes their non-coalescing, non-wetting behaviour. We also draw parallels with the vibration-induced stability of an inverted pendulum.

2.3 Vibro-Levitation of Droplets

Water droplets are seen to float momentarily on the surface of water and then coalesce into the bulk fluid. Sometimes they emit a smaller droplet as a result of coalescence, which then undergoes the same fate as the parent droplet.²⁷ This phenomenon is called coalescence cascade. Such non-coalescing droplets were noticed as early as 1881 when Reynolds studied the influence of surface impurities on this peculiar behaviour of droplets. He concluded that a pure liquid surface is required for droplets to float over it.²⁸

Walker demonstrated by a simple experiment that droplets of an aqueous soap solution can levitate in a non-coalescent state above a vibrating bath of the same bulk solution. The droplets could levitate indefinitely if standing waves (Faraday instabilities) were set up on the bulk liquid surface.²⁹ Recently this phenomenon has attracted the attention of researchers once again. Couder *et al.*³⁰ demonstrated that silicone oil droplets could be levitated indefinitely over a sinusoidally vibrating ($A \cos \Omega t$) bath of oil. While Walker noticed indefinitely levitating droplets only in the presence of standing waves on the bulk liquid surface, Couder *et al.* were able to obtain indefinitely levitating droplets over a stable liquid surface. In both cases, vibration stabilizes the droplet in a non-coalescing state above the liquid bath. Therefore we refer to such a droplet as a vibro-levitating droplet.

A vibro-levitating droplet is in a repetitive cycle of impact and bounce-off at the liquid surface. If its radius is larger than the capillary length ($\sqrt{\gamma/\rho g}$, where γ and ρ are the liquid surface tension and density respectively) the droplet undergoes continuous deformation from spherical to oblate and prolate shapes, which may setup oscillations along the droplet surface.³¹ When the droplet impacts the liquid surface, the kinetic energy of the droplet is dissipated into surface energy by flattening of the droplet, oscillations of the droplet, and viscous damping in the air film between the droplet and the liquid surface.³² The droplet does not coalesce with the bulk liquid surface so long as the thin air film is replenished and stabilized due to the applied vibrations.

The vibro-levitating droplets produced weak surface waves every time they bounced off the liquid surface. These surface waves grew larger in amplitude when the amplitude A of the applied vibration was increased. At a critical value of A near the onset of Faraday instabilities, the levitating droplets started to move in seemingly random horizontal trajectories over the vibrating liquid surface. This motion is due to the interaction between the surface wave and the levitating droplet on each impact. Couder *et al.* called the system of the droplet and its associated wave a “walker”.¹³ These walkers can interact and orbit with each other, and can also form self-assembled ordered patterns.^{14,33,34} Within a certain range of frequencies, the vibro-levitating droplets can roll over the liquid bath due to internal rotation.³⁵

Vibro-levitating droplets have some parallels with the wave-particle duality from quantum mechanics.³⁶ The droplets illustrate several quantum mechanical phenomena such as single-particle diffraction, quantized orbits, and tunnelling.³⁷⁻³⁹ But this comes with a caveat that there is a great difference between the physics in the macro and subatomic domains. Discussion of these topics is beyond the scope of this chapter.

There are models which describe the levitation and horizontal motion of these non-coalescent droplets.^{30,40-42} The effect of bouncing droplets is thought to be similar to the acoustic levitation due to non-linear viscosity in a thin film which leads to hysteresis. However, a detailed model of such effects remains quite complex. In the following section, we suggest a simple analogy between the vibro-levitating droplets and the inverted pendulum.